Available online at www.sciencedirect.com
SCIENCE DIRECT®
Journal of Power Sources 122 (2003) 67–76
JOURNAL OF POWER SOURCES
www.elsevier.com/locate/jpowsour

Comparison of the capacity fade of Sony US 18650 cells charged with different protocols

G. Sikha, P. Ramadass, B.S. Haran, R.E. White, Branko N. Popov*

Department of Chemical Engineering, Center for Electrochemical Engineering, University of South Carolina, Columbia, SC 29208, USA

Received 12 December 2002; accepted 20 December 2002

Abstract

A new varying current decay (VCD) protocol, which charges the Li-ion battery at a faster rate, was developed. The performance of the battery charged using the VCD protocol was compared with the performance of batteries charged with conventional constant current–constant voltage (CC–CV) and constant voltage (CV) protocols. The destructive physical analysis tests at the end of 150 cycles indicated higher impedance for the cells cycled using the VCD protocol compared to the cell charged using the conventional (CC–CV) mode. The observed increase of the impedance was due to a small increase of the potential above the cut-off value of 4.2 for short times. A complete capacity fade material balance as a function of number of cycles was performed in order to account for the total capacity loss due to different charging protocols used. The loss of primary active material (Li^+), the secondary active material ($LiCoO_2$/carbon) and the rate capability losses were determined for Sony US 18650 Li-ion cells and compared for different charging protocols.

Keywords: Sony US 18650 cells; Protocols; Li-ion

1. Introduction

Lithium ion intercalation (deintercalation) in both the positive and negative electrode controls the battery charging and discharging rate [1–5]. Since these processes are diffusion controlled and slow, it is necessary that a low charging rate is used. However for certain applications where rapid recharging is necessary, the conventional constant current–constant voltage (CC–CV) mode of charging (low rate constant current until the potential reaches to a predetermined cut-off potential followed by float charging at the cut-off potential until the current drops to a very low preset value) would not be favorable. For fast charging, a constant voltage (CV) charging mode is the only alternative. However, the failure of the cell using this mode is very high due to very high currents in the initial stages of charging. This charging mode continuously maintains the potential at the cut-off value of 4.2 which is highly detrimental to the life of the cell due to various limitations such as electrolyte oxidation, active material degradation, etc. [1]. Also, this mode requires very robust and expensive chargers capable of delivering very high currents in the initial stages of charging.

Chung et al. [6] showed that charging with linearly descending current results in reduction of charging time as compared with the constant current charging to the same state of charge (SOC). Our preliminary studies indicated that using this protocol the reduction of time factor as stated could be accomplished only at the expense of overcharging the cell, which drastically reduces the cycle life of the battery.

In this work, a varying current decay (VCD) with time, as a mode for a charging lithium ion battery was developed which charges the battery faster than CC–CV mode. Also, the performance of the battery charged using the VCD protocol was compared with the performance of batteries charged with conventional CC–CV and CV protocols. A complete capacity fade material balance as a function of number of cycles was undertaken in order to account for the total capacity loss due to different charging protocols. Destructive analysis of the cycled cells was performed to analyze the effects of various charging modes on individual electrodes.

2. Experimental

All studies were carried out on Sony US 18650 Li-ion cells (obtained from Comdev Inc.) with a 1.4 Ah rated capacity at room temperature. The cell characteristics are shown

* Corresponding author. Tel.: +1-803-777-7314, fax: +1-803-777-8265.
E-mail address: popov@engr.sc.edu (B.N. Popov).

0378-7753/03/$ – see front matter © 2003 Elsevier Science B.V. All rights reserved.
doi:10.1016/S0378-7753(03)00027-2

Table 1
Cell characteristics of commercial Sony US 18650 lithium ion batteries

Characteristics	Positive $LiCoO_2$	Negative carbon
Mass of the electrode material (g)	13.5	6.9
Mass of active material (g)	11.4	6.6
Geometric area (both sides) (cm^2)	497.6	536.8
Loading on one side (mg/cm^2)	23.0	12.2
Dimensions of the electrode (cm^2)	46.5 × 5.35	47.5 × 5.65
Thickness of current collector (μm)	29	24

in Table 1. The following charging protocols were used to charge the batteries.

(a) In the case of the VCD protocol, the battery was charged with a 5 A short pulse until the potential reached a cut-off value of 4.2 V, followed by the current decay protocol for a total time of 5400 s. The current decay protocol follows the empirical equation $I(t) = (I_0 + k_1 t^{1/2})/(1 + k_2 t^{1/2} + k_3 t)$ where k_1, k_2, k_3 are arbitrary constants, I_0 is the initial current and t the instantaneous time. Under these conditions, the cell was approximately charged to 98% of its nominal capacity.
(b) The CC–CV protocol was performed using a constant current of 0.9 A (current equivalent to the average current for the VCD protocol) until the potential reached the cut-off value of 4.2 V. This was followed by a float charge at 4.2 V for a time necessary to charge the battery to an approximately 98% state of charge. This time was fixed for further cycling.
(c) In the case of the CV protocol, the cell was potentiostatically-controlled at 4.2 V until the battery was charged to an approximately 98% state of charge. The corresponding charging time was used as a fixed time for further cycles.

For all the above cases the discharge was done at 1 A until the voltage of the battery reached 2.5 V.

An Arbin Battery Cycler (BT-2000) was used to charge and discharge the batteries. Electrochemical characterization studies were done using the Solartron SI 1255 HF frequency response analyzer coupled with a Potentiostat/Galvanostat model 273A. The EIS studies were done for fresh and cycled cells in the completely charged and discharged states. The dispersion data for a 5 mV ac perturbation over the frequency range of 10 mHz to 0.1 MHz were analyzed. Rate capability studies were done for the fresh and the cycled full-cells to determine the maximum capacity that can be delivered by the battery. A destructive cell analysis was performed on both the carbon and the $LiCoO_2$ electrodes. The cells were cut open in a glove box filled with ultra pure argon (National Gas and Welders Inc.). Discs of radius ca. 1.2 cm were punched from the electrode sheet ($LiCoO_2$ or carbon) and a three electrode set-up using a T-shaped polypropylene cell with stainless steel current collectors was used for the half-cell studies. High purity lithium discs (LectroMax 100) were used both as counter and reference electrodes. The electrolyte solution was a 1 M solution of $LiPF_6$ in 1:1 mixture of ethyl carbonate (EC)/dimethyl carbonate (DMC) with a polypropylene separator. The half-cells were allowed to attain equilibrium until the voltage stabilized. To analyze the loss of capacity due to secondary material loss ($LiCoO_2$ or carbon), the individually prepared half-cells were cycled at a low rate to find the available capacity of the materials after prolonged cycling. EIS studies were also done on half-cells to analyze the individual resistance contributions. Surface analysis using scanning electron microscope (SEM) was done to analyze the morphological features of the electrodes after prolonged cycling.

3. Results and discussion

The linear current decay (LCD) charging protocol follows an empirical equation of the form $I = I_0 - k_1 t$. The slope k_1 and the initial current I_0 should be chosen in this protocol so that the voltage profile does not pass the cut-off potential of 4.2 V. In fact, k_1 determines the criteria for overcharging. Thus, an optimum slope (k_1) must be chosen in order to prevent overcharging and to attain a maximum utilization (the ratio of charge capacity obtained at any instant to the nominal charge capacity). Experimental charging curve presented in Fig. 1 shows the deficiencies of the LCD protocol for optimized values of k_1 and I_0. At the end of charging, the current decreases to a very low value, which is not sufficient to maintain the potential at the cut-off value of 4.2 V. Thus a complete charging of the battery cannot be accomplished.

To overcome this problem and to charge the battery completely, we developed a modified linear current decay (MLCD) protocol. The current expression used in this case was of the form $I = I_0 - k_1 t - k_2\sqrt{t}$. As shown in Fig. 2, the $k_2\sqrt{t}$ term in this protocol corrects the current profile shown in Fig. 1. The current in Fig. 2 does not decrease as fast as the current profile observed in the case of the LCD protocol. Using MLCD protocol it is possible to charge the battery to a 100% state of charge at a faster rate. From the voltage profile in Fig. 2 it can be noted that the only part where utilization can be tapped at a faster rate is the initial part of the current profile. As shown in Fig. 2, initially the voltage increases slowly to the cut-off potential. This is a key time reduction factor if one wants to develop a rapid charging protocol. Thus, instead of a continuously decreasing current function, a short high current pulse was triggered at the start until the voltage reaches a value close to the cut-off potential and then the current decay profile was initiated. In Fig. 3, the new (VCD) protocol initially applies a short current pulse of 5 A, which is followed by a decay in the current of the form $I(t) = (I_0 + k_1 t^{1/2})/(1 + k_2 t^{1/2} + k_3 t)$. Using the VCD protocol one reaches the cut-off potential as soon as charging starts and then maintains the potential near the cut-off value throughout the charging period. Fig. 4 shows that the VCD protocol charges the battery faster than the conventional CC–CV or the CV mode.

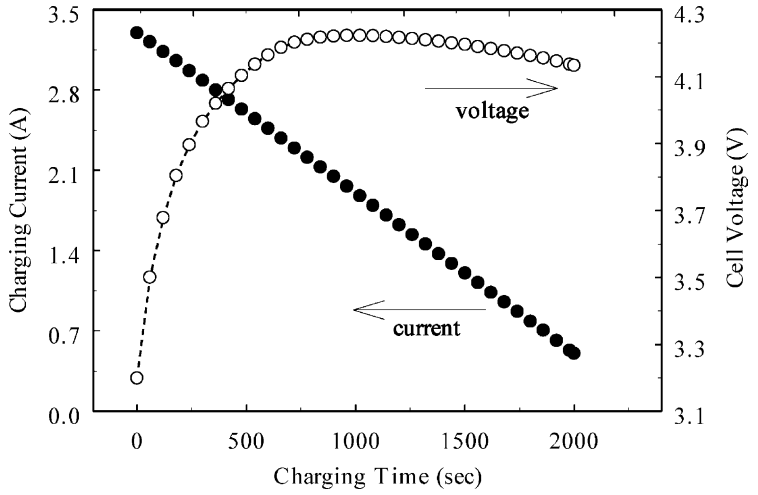

Fig. 1. Current–voltage relationship for the linear current decay protocol (LCD).

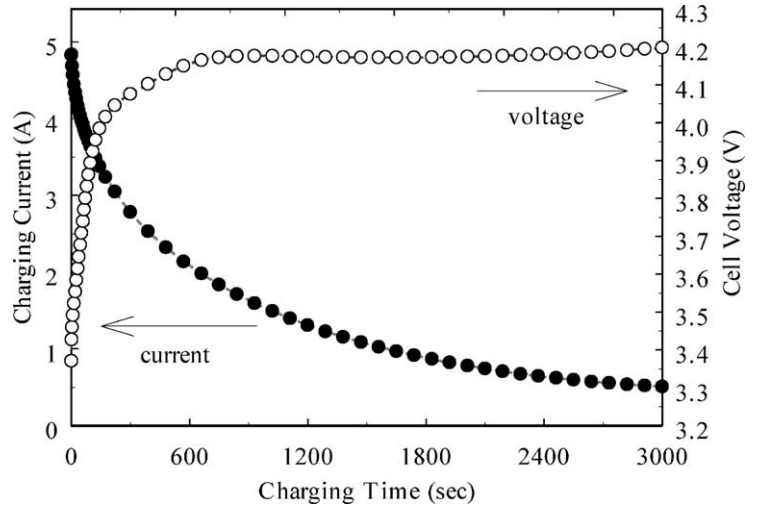

Fig. 2. Current–voltage relationship for the modified linear current decay protocol (MLCD).

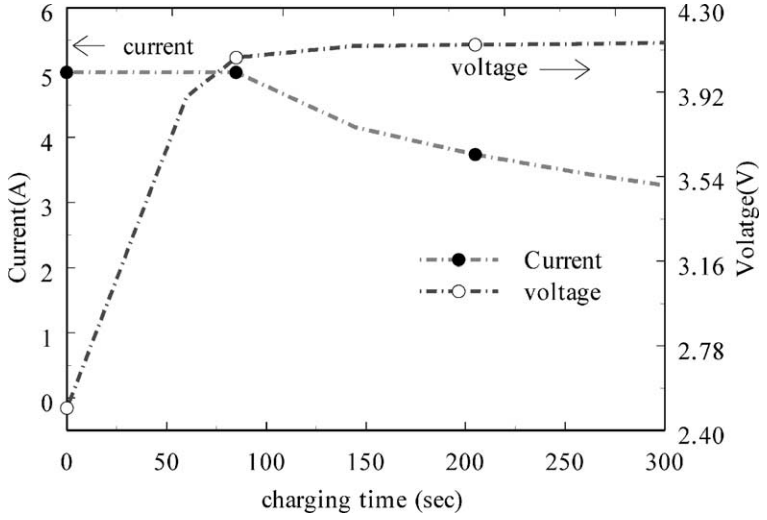

Fig. 3. Current–voltage relationship for the VCD protocol.

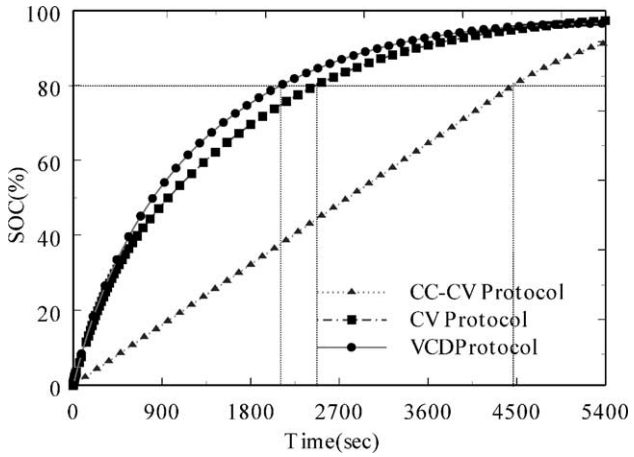

Fig. 4. Utilization comparison for CC–CV, CV and the VCD protocol.

Next, the cycling performance (capacity fade) of the batteries charged with VCD protocol was compared with those charged using conventional charging protocols. Three cells were cycled for each of the above protocols. Fig. 5 shows the charging curves for the CC–CV protocol at the end of various cycle numbers. In the case of the CC–CV protocol as the cell is cycled more, the time in which the cell remains in the constant current part decreases and most of the charging is carried out through the float voltage part. The utilization dropped from 98% in the first cycle to 90.25% at the end of 150 cycles corresponding to a charge capacity of 1.263 Ah. Table 2 presents the decrease in percentage of CC time and the decrease in charge capacity as a function of cycle number. The observed decrease of charge capacity is due to the combined loss of primary active material (Li^+), secondary active material ($LiCoO_2$/carbon) and the rate capability losses. The cell reaches the cut-off potential at shorter time intervals with cycling due to the poor rate capability on both positive and negative electrodes. The rate capability losses result from the formation of oxide films on

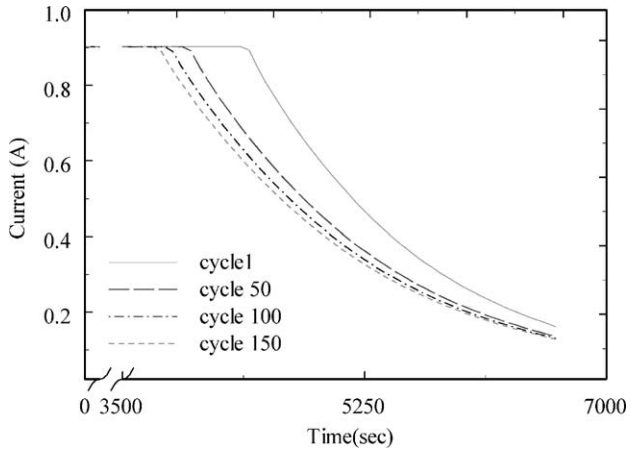

Fig. 5. Charge curves for the cells cycled using CC–CV protocol at the end of 1, 50, 100 and 150 cycles.

Table 2
Variation of CC time and charge capacity with cycling for CC–CV protocol

	Cycle number			
	1	50	100	150
CC time (s)	4356	3935	3805	3720
Percentage of CC time decrease	0	9.66	12.65	14.60
Charge capacity (Ah)	1.367	1.292	1.271	1.263
Utilization (%)	97.42	92.28	90.78	90.25

both electrodes through which Li^+ intercalates at a slower rate.

In the case of the CV charging protocol, the cell has to reach the cut-off potential immediately, resulting in very high initial currents. However as cycling progresses lower peak currents are sufficient to take the cell potential to the cut-off value because of the resistance developed. Table 3 presents the capacity of the cell, utilization percentage and also the decrease in the peak current with cycling using the CV protocol.

In the VCD protocol mode, the charge curves remain almost the same with cycling except in the initial part where the duration of the pulse current goes on decreasing with cycling as shown in Fig. 6. The pulse current is similar to the constant current in the CC–CV protocol and the duration of the constant current part decreases with cycling due to rate capability losses. The current profile in the VCD protocol starts when the pulse current ends. Table 4 shows

Table 3
Variation of utilization and peak current for CV protocol

	Cycle number			
	1	50	100	150
Peak current (A)	13.19	12.17	11.82	10.25
Charge capacity (Ah)	1.381	1.311	1.283	1.249
Utilization (%)	98.57	93.49	91.64	89.21

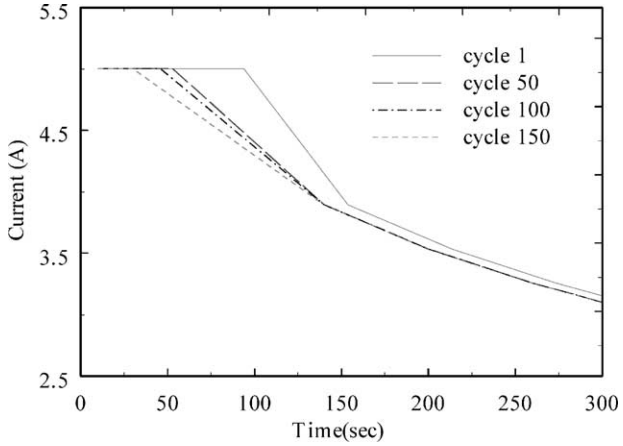

Fig. 6. Charge curves for the cells cycled using the VCD protocol at the end of 1, 50, 100 and 150 cycles (the figure shows the decrease in the initial pulse time with cycling).

Table 4
Variation of CC time and charge capacity with cycling for the VCD protocol

	Cycle number			
	1	50	100	150
CC time (s)	93	56	45	28
Charge capacity (Ah)	1.377	1.311	1.289	1.254
Utilization (%)	98.30	93.64	92.07	89.67

the reduction in the pulse time with cycling and also the decrease in the utilization with cycling in the VCD protocol.

Fig. 7a–c show the discharge curves obtained at the end of 1, 50, 100 and 150 cycles for the CC–CV, CV and VCD protocols, respectively. Although the capacity fade differed with the protocols, the nature of the discharge curves remained the same. They did not show a drastic change of the initial voltage drop, nor a shift of the plateau to a lower potential indicating that the ohmic and the polarization resistance was not changed substantially during cycling. As shown in Fig. 7c, the VCD protocol showed a lower capacity fade when compared with the capacity fade observed for the batteries cycled using the CV protocol despite the fact that both protocols were charged to the same state of charge for the same period of time. Note that the CC–CV protocol showed a lower capacity fade. However, these batteries were charged for longer period of time to attain the same state of charge as of those charged using VCD or CV protocols in the first cycle. The results indicated that high capacity fade observed for batteries charged using the CV protocol is due to very high currents used to charge the battery initially. Table 5 compares capacity fade for the three protocols used in this study. For the CC–CV protocol the total charging time in the constant current mode decreases with cycling. The charge lost during the constant current time is slightly higher than the charge gained in the additional constant voltage time in each cycle. In the case of the VCD protocol, the decaying charging profile remains the same throughout cycling. However, the reduction in available charge was due to the decrease in the pulse time (as the cell reaches the cut-off quicker with cycling) as cycling progresses. Since during the current decay part of the profile remains unchanged with cycling, a slight increase of the potential was observed immediately after the pulse current part was over. It appears only for a few seconds at the onset

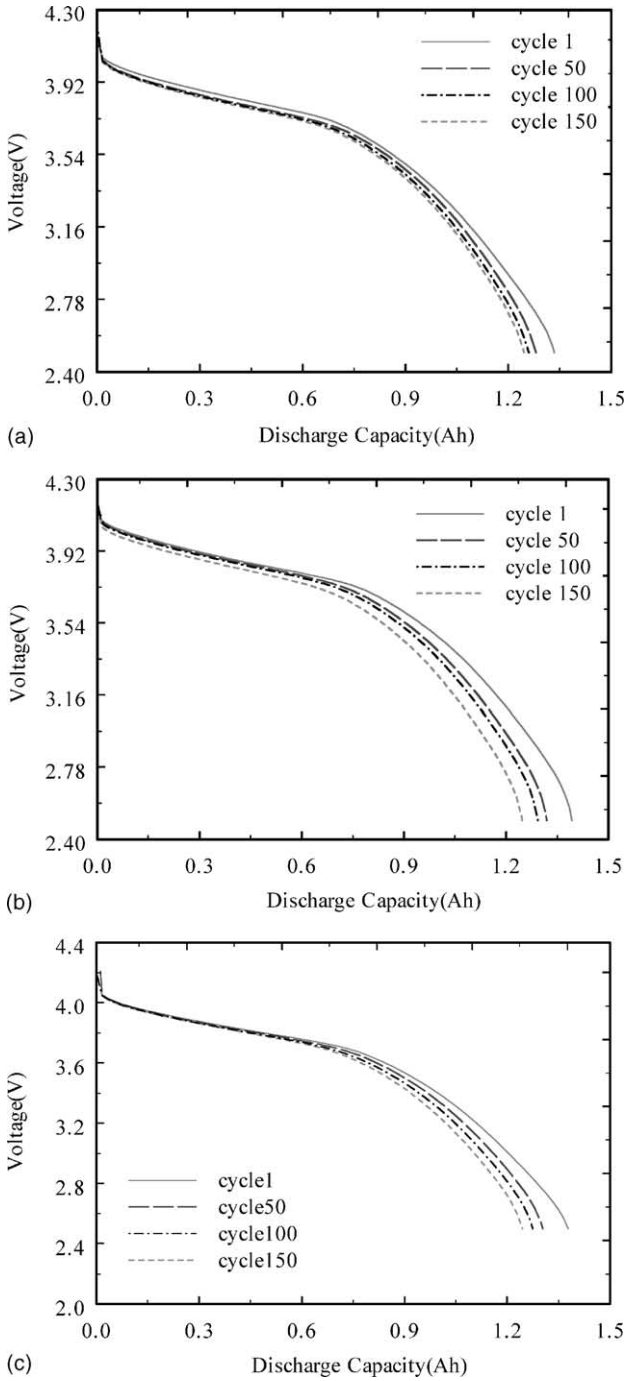

Fig. 7. (a) Discharge curves for the cells cycled using the CC–CV protocol at the end of 1, 50, 100 and 150 cycles; (b) discharge curves for the cells cycled using the CV protocol at the end of 1, 50, 100 and 150 cycles; (c) discharge curves for the cells cycled using the VCD protocol at the end of 1, 50, 100 and 150 cycles.

Table 5
Capacity fade comparison for the three protocols after 50, 100 and 150 cycles

Protocol type	Percentage capacity fade		
	50	100	150
CC–CV protocol	4.06	5.61	6.64
CV protocol	5.24	7.51	10.42
VCD protocol	5.37	7.54	9.506

of the current profile. This voltage rise immediately reverts back to the cut-off potential for the rest of the charging time. However, an increase in the voltage peak is also observed as cycling progresses. This phenomena causes higher capacity fade to be observed in case of batteries charged with the VCD protocol compared with the CC–CV protocol. It

is unclear whether the potential rise is due to the increase of resistance on the carbon anode with cycling or the cell is overcharged. In the case where the cell is overcharged, the voltage spike will cause lithium deposition on the anode and consequently an increase of the capacity fade due to a loss of the primary active material, Li^+.

3.1. Impedance analysis

Impedance measurements were carried out for both full-cells and for the individual electrodes. For half-cell studies, the electrodes were taken from the cells after 150 cycles. The goal was to determine whether after various charge/discharge cycles there is an increase in resistance with cycling that could be related to capacity fade. Fig. 8 presents the cell impedance for fresh cells at the 0 and 100% state of charge. It was found that for a fresh cell, the impedance decreases with increase in SOC. This is an expected feature of Li-ion cells because the transition metal oxides are good conductors. Li^+ intercalation through the interstitial sites of the transition metal oxide makes it semiconductive. However on the negative electrode Li^+ intercalation increases the conductivity of the matrix [7].

Fig. 9 shows the full-cell impedance data (at zero state of charge) at the end of 150 cycles for the cells cycled with various charging protocols. The results are compared with the impedance data observed for the fresh cell. A slightly higher impedance is seen for the cells cycled with the VCD protocol. This may result from additional film formation due to the electrolyte oxidation during the spike in the potential, which was discussed above immediately after the pulse current part of the VCD protocol was over. Impedance studies of the full-cell gave only the overall cell resistance. Thus, the contribution of positive and negative electrodes to the overall cell resistance cannot be determined unless half-cell studies were conducted for individual electrodes.

Fig. 10a and b shows the Nyquist plots of fresh and cycled $LiCoO_2$ electrodes at 0 and 100% SOC respectively.

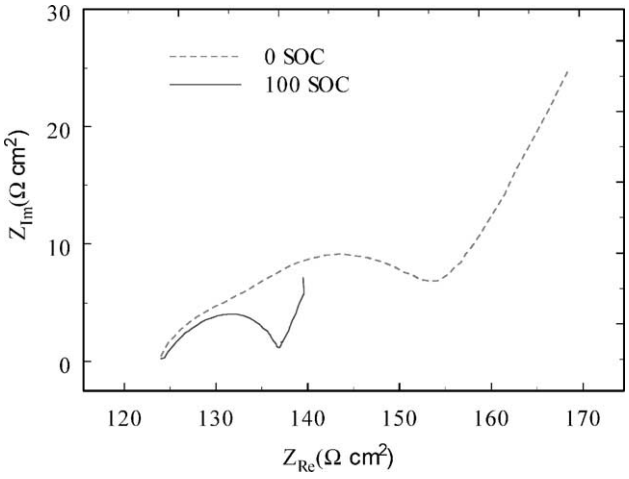

Fig. 8. Impedance for a fresh cell at 0 and 100% state of charge.

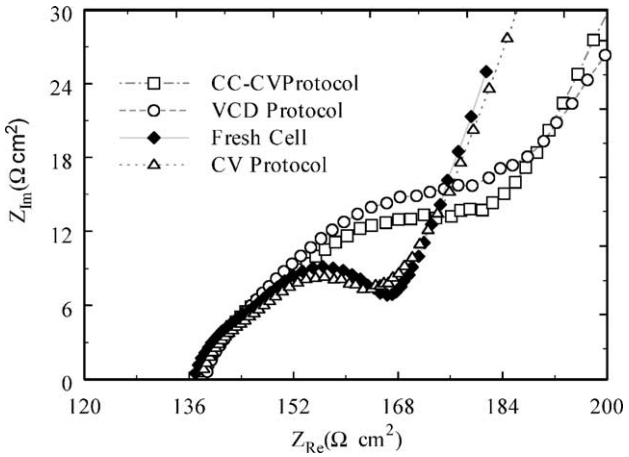

Fig. 9. Full-cell impedance for the cells cycled with various charging protocols at 0% SOC at the end of 150 cycles.

The size of all semicircles increased drastically with cycling, indicating an increase in electrode resistance. However, the VCD protocol showed higher impedance in both the lithiated and delithiated states when compared to that of the

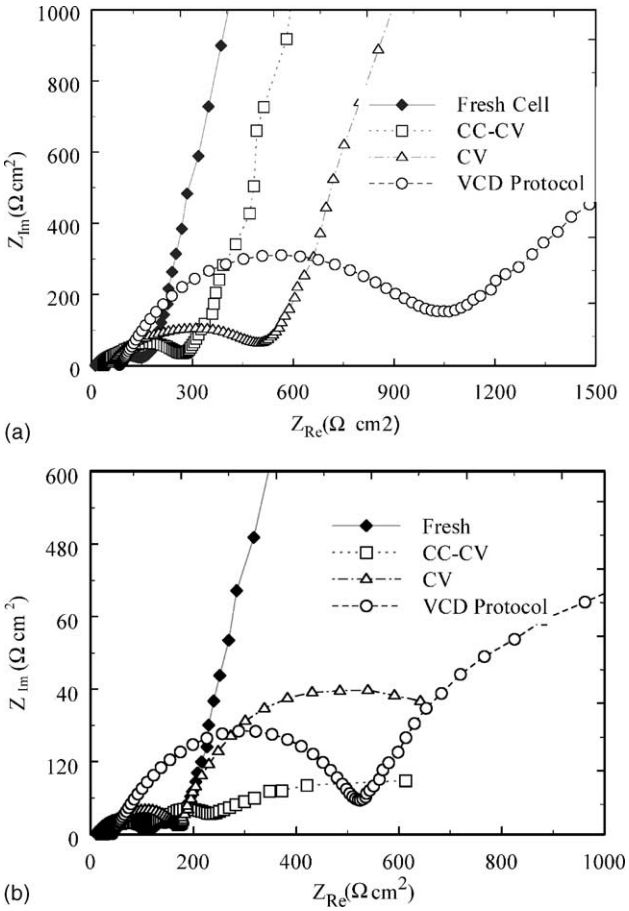

Fig. 10. (a) Nyquist plots for completely lithiated half-cell $LiCoO_2$ taken from full-cells cycled with different protocols; (b) Nyquist plots for completely delithiated half-cell $LiCoO_2$ taken from full-cells cycled with different protocols.

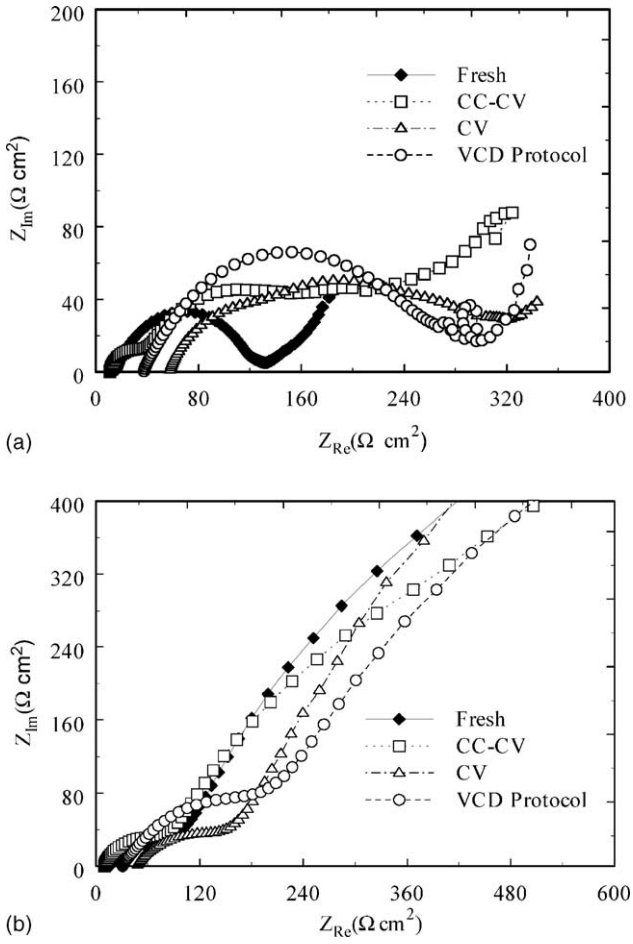

Fig. 11. (a) Nyquist plots for completely lithiated half-cell carbon electrode taken from full-cells cycled with different protocols; (b) Nyquist plots for completely delithiated half-cell carbon electrode taken from full-cells cycled with different protocols.

other protocols. The observed increase of the impedance of the $LiCoO_2$ electrode (mid frequency region) in the case of the VCD protocol suggests a possible electrolyte oxidation leading to a film formation which occurs during the slight increase of the potential over the cut-off value observed immediately after the pulse current part of the VCD protocol was over.

Fig. 11a and b shows Nyquist plots of fresh and cycled carbon electrodes at 100 and 0% SOC, respectively. The resistance contributions from the carbon electrode were always smaller than that of the positive electrode. Although there was an increase in the impedance of the carbon electrode, it was uniform for all protocols and thus it can be concluded that the charging mode does not affect the carbon electrode. From the analysis of impedance data and charge and discharge curves it is clear that the increase in internal resistance causes a decrease in energy efficiency with cycling [8]. The rate capability of the cell becomes poor due to a decrease in the diffusion rate in the solid phase of the electrode.

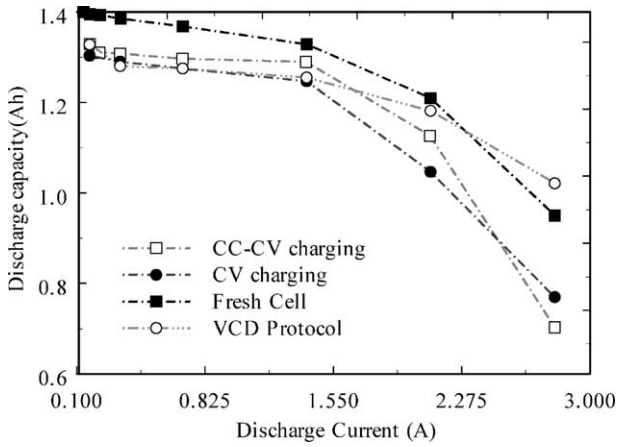

Fig. 12. Rate capability studies for cells cycled using the three protocols at the end of 150 cycles. The different rates of discharge are C/8, C/4, C/2, C, 2C, and 3C.

3.2. Rate capability studies

Fig. 12 presents the rate capability (discharge capacity versus discharge current) estimated for fresh cells and for those cycled for 150 cycles. The cells that were charged with different charging protocols were discharged at the rates of C/8, C/4, C/2, C, 2C and 3C. Based on the data presented in Fig. 12 it was observed that after 150 cycles the full-cell shows an increase in the actual capacity at very low discharge rates compared with what was observed at normal rates. The results also indicate that the film resistance formed on the electrode surface impedes the diffusion of Li^+ ions into the electrode and thus a very low rate of discharge is necessary to obtain the remaining capacity. This fact also indicates that Li^+ ion loss during cycling is not the crucial contribution to the capacity fade mechanism.

3.3. Quantitative capacity fade analysis from T-cells and overall capacity balance

The three most significant parameters that we consider to cause the capacity fade loss (Q) are the rate capability losses denoted as Q_1, secondary active material losses denoted as Q_2 and the primary active material losses which corresponds to loss of Li^+ denoted as Q_3 [9]. Thus, the capacity fade balance can be represented as the sum of Q_1, Q_2, and Q_3. Our objective was to estimate each of the above capacity losses and to correlate them with the charging protocols used in this study.

Capacity fade due to active material degradation can be estimated from the intrinsic capacity measurements. T-cells were made from both positive and negative electrodes as working electrodes with Li metal being the counter and the reference electrode in each case. Low rate lithiation and delithiation experiments were done with these half-cells with carbon and $LiCoO_2$ electrodes that were cycled using different protocols as working electrodes and compared with the fresh material. Next, the available capacity of the working

electrode was measured and scaled up to the original full-cell electrode geometry. This, when compared against the fresh cell capacity, would give the value for the secondary active material losses (Q_2). Since the material is cycled with excess of Li^+, any loss in the capacity should be related to the inefficiency of the secondary active material. The capacity of the limiting electrode between carbon and $LiCoO_2$ will determine the value of Q_2.

The value of Q is the full-cell discharge capacity loss at the end of 150 cycles estimated for each protocol and corresponds, as discussed above, to the overall loss of capacity in the cell. To estimate the value of Q_1, the full-cell after being cycled for 150 cycles was discharged at a very low rate (C/10) to eliminate the contribution of the rate capability losses to the total capacity fade of the battery. In other words at low rate it was possible to extract the maximum capacity from the battery. This difference between the apparent capacity measured and the actual capacity at low

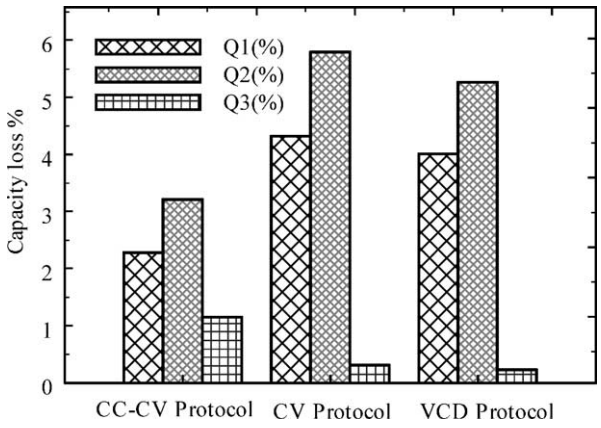

Fig. 13. Rate capability losses (Q_1), secondary active material losses (Q_2) and primary active material losses (Q_3) for the three charging protocols.

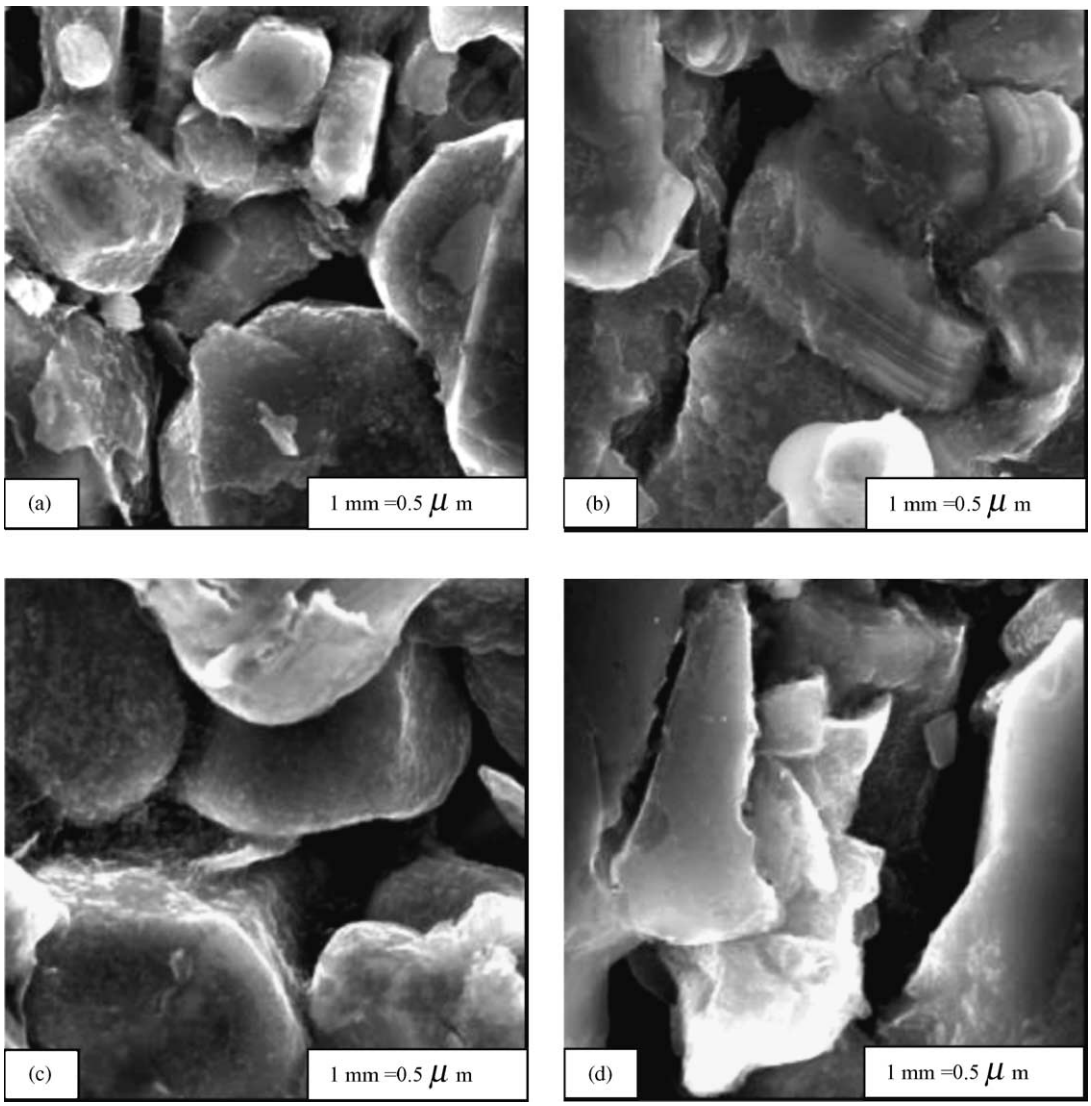

Fig. 14. Micrographs of $LiCoO_2$ cathodes: (a) fresh electrode; (b) charged using CC–CV protocol at the end of 150 cycles; (c) charged using constant voltage protocol at the end of 150 cycles; (d) charged using the VCD protocol at the end of 150 cycles.

rates contribute to Q_1. Making a charge balance by subtracting Q_1 and Q_2 from the total capacity fade loss estimated (Q) one could determine the value of Q_3, which is attributed to the primary material loss.

Fig. 13 shows the quantitative comparison of the values of Q_1, Q_2 and Q_3. The results indicated that the loss of lithium ions does not dominate the overall capacity fade. In this case the carbon electrode limits the cell capacity as seen in the individual capacity fade analysis after 150 cycles. The capacity fade is highest for the cells cycled using the constant voltage protocol. The cells also showed an increased loss in capacity due to rate capability and carbon material loss in the case of the VCD and CV protocols. Repeated film formation on the carbon electrode could be one of the reasons for the decreased lithiation capacity and reduced rate capability. Cycling the cell using higher rates of charging aggravates the problem and leads to large capacity decay.

3.4. SEM studies

To analyze the surface morphological changes, electron micrographs were obtained for positive and negative materials taken from cells cycled with different protocols. As can be seen in Fig. 14, the fresh cell has well rounded $LiCoO_2$ particles with an average diameter of 10–20 μm. While there is not much of a difference between the surfaces of the CC–CV cycled, CV cycled and the fresh $LiCoO_2$ electrode, the cells cycled using the VCD protocol showed cracks in most areas of the sample. This indicates that a rapid intercalation or deintercalation of the Li^+ ions into and from the $LiCoO_2$ matrix created a heavy stress and volume expansion in the cathode material [10,11].

In the case of the carbon electrodes as seen in Fig. 15, the cells cycled using the VCD protocol and the CV protocol show an agglomerated film formation while the fresh carbon electrode has clear and distinct particles. This is due to the increased film formation due to the products formed as a result of Li^+/solvent reactions on the surface of the carbon electrode [1]. Any increase in the electrode resistance of the anode is very detrimental because on further cycling, the half-cell $LiCoO_2$ potential will rise over the initial set cut-off potential [7]. This triggers the side reactions that occur when the electrode is overcharged. The presence of the surface film shown in Fig. 15 on the carbon electrode correlates well

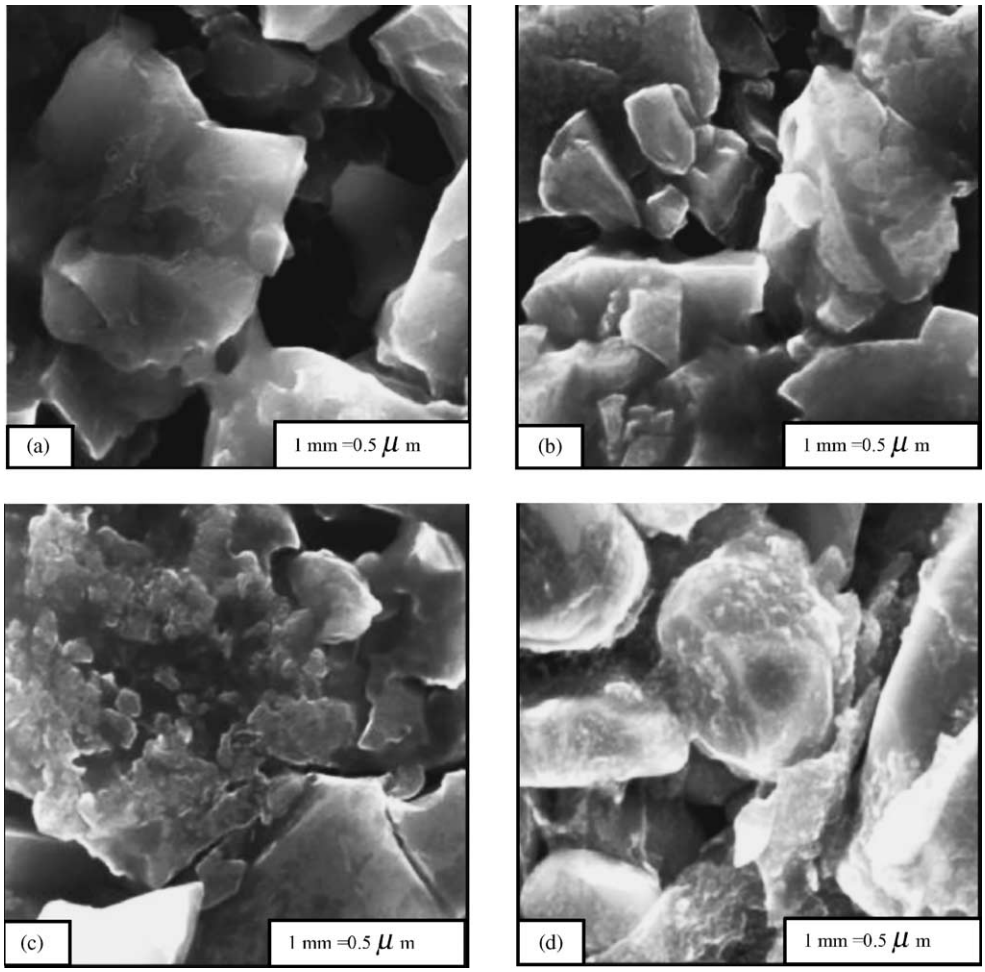

Fig. 15. Micrographs of carbon anodes: (a) fresh electrode; (b) charged using CC–CV protocol at the end of 150 cycles; (c) charged using constant voltage protocol at the end of 150 cycles; (d) charged using the VCD protocol at the end of 150 cycles.

with the fact that a high rate capability loss exists for both CV and VCD protocol.

4. Conclusions

The capacity of a Li-ion battery depends on the protocol used to charge the battery. The short time during which the current is very high while charging using the CV protocol (taking the system from zero state of charge to the cut-off potential) is responsible for the increased capacity fade of the CV protocol compared to the VCD protocol. Although the VCD protocol has a slight overcharge on cycling, better optimization of the current profile could lead to faster charging and lower capacity fade if this type of protocol is used to charge the battery. The possibility of overcharging the positive electrode beyond the cut-off value in a potentiostatically-controlled cell is very high due to the possible increase in the negative electrode potential with cycling. However, one can optimize the VCD protocol so that the potential never increases beyond the cut-off potential. This would result in a very safe mode for charging the battery at a faster rate. As was seen in the quantitative capacity fade analysis, the secondary active material in the negative electrode fades faster than $LiCoO_2$ and hence this electrode dominates the capacity fade of the battery. The rate capability loss is proportional to the value of the average current used. Thus, one cannot avoid this apparent increase of the capacity fade when the battery is charged at fast rates. However, the material degradation can be eliminated by using an optimized current profile, which would keep the potential always below the cut-off value, thereby ensuring minimal overcharging.

Acknowledgements

The authors are thankful for the financial support provided by National Reconnaissance Organization (NRO) under Contract No. NRO-00C-0134.

References

[1] P. Arora, R.E. White, M. Doyle, J. Electrochem. Soc. 145 (10) (1998) 3647.
[2] P. Ramadass, A. Durairajan, B. Haran, R.E. White, B.N. Popov, J. Electrochem. Soc. 149 (1) (2002) A54.
[3] D. Aurbach, B. Markovsky, I. Weissman, E. Levi, Y. Ein-Eli, Electrochim. Acta 45 (1999) 67.
[4] M. Doyle, J. Newman, A.S. Gozdz, C.N. Schmutz, J.-M. Taracson, J. Electrochem. Soc. 143 (6) (1996) 1890.
[5] M. Broussley, P. Biensan, B. Simon, Electrochim. Acta 45 (1999) 3.
[6] S.K. Chung, A.A. Andriiko, A.P. Mon'ko, S.H. Lee, J. Power Sources 79 (1999) 205.
[7] D. Zhang, B. Haran, A. Durairajan, R.E. White, Y. Podrazhansky, B.N. Popov, J. Power Sources 91 (2000) 122.
[8] P. Ramadass, B. Haran, R.E. White, B.N. Popov, J. Power Sources 112 (2002) 606.
[9] P. Ramadass, B. Haran, R.E. White, B.N. Popov, J. Power Sources 112 (2002) 614.
[10] H. Wang, Y. Jang II, B. Huang, D.R. Sadoway, Y.-M. Chiang, J. Electrochem. Soc. 146 (2) (1998) 473.
[11] J. Li, E. Murphy, J. Winnick, P.A. Kohl, J. Power Sources 102 (2001) 294.